

AIAA 2002-0971

Model-Based Control of Cavity
Oscillations – Part 1: Experiments

D.R. Williams

Illinois Institute of Technology, Chicago IL

C. Rowley

Princeton University, Princeton NJ

T. Colonius, R. Murray, D. MacMartin

California Institute of Technology, Pasadena CA

D. Fabris

Santa Clara University, Santa Clara CA

Chicago, IL

J. Albertson

U.S. Air Force Academy CO

MODEL-BASED CONTROL OF CAVITY OSCILLATIONS PART 1: EXPERIMENTS¹

David R. Williams^{a,2} Clancy W. Rowley^b Tim Colonius^c Richard M. Murray^c
Douglas G. MacMartin^c Drazen Fabris^d Julie Albertson^e

^a Fluid Dynamics Research Center, Illinois Institute of Technology, Chicago, IL 60616

^b Mechanical & Aerospace Engineering, Princeton University, Princeton, NJ 08544

^c Division of Engineering and Applied Science, California Institute of Technology, Pasadena, CA 91125

^d Mechanical Engineering, Santa Clara University, Santa Clara, CA 95053

^e Aeronautics Laboratory, U.S. Air Force Academy, CO

δ_{ω} = Vorticity thickness $(U_2 - U_1)/dU/dy|_{\max}$

Abstract

An experimental investigation of acoustic mode noise suppression was conducted in a cavity using a digital controller with a linear control algorithm. The control algorithm was based on flow field physics similar to the Rossiter model for acoustic resonance. Details of the controller and results from its implementation are presented in the companion paper by Rowley, et al.¹ Here the experiments and some details of the flow field development are described, which were done primarily at Mach number 0.34 corresponding to single mode resonance in the cavity. A novel method using feedback control to suppress the resonant mode and open-loop forcing to inject a non-resonant mode was developed for system identification. The results were used to obtain empirical transfer functions of the components of resonance, and measurements of the shear layer growth for use in the design of the control algorithm.

Nomenclature

D = Cavity depth
f = Frequency
L = Cavity length
M = Freestream Mach number
 p_1 = Wind tunnel static pressure
q = Dynamic pressure $\frac{1}{2} \rho U^2$
r = U_1/U_2 shear layer velocity ratio
St = Strouhal number, fL/U
U = Freestream speed
 U_2 = Velocity of high speed side of shear layer
 U_1 = Velocity on low speed side of shear layer

1. Introduction

Over the last few years new methods for controlling acoustic tones in aircraft weapons bays have received an increasing amount of attention. A variety of different active and passive control techniques have been used to suppress acoustic tones in cavities under compressible flow conditions, in an attempt to improve upon the noise suppression provided by conventional fences and spoilers. Without any suppression technique sound pressure levels of cavity tones often exceed 160 dB, even at moderate subsonic Mach numbers^{2,3}. The large amplitude tones may lead to structural fatigue in aircraft components and the ordnance carried on board. In addition to structural fatigue, measurements of drag have shown 250% increase in cavity drag as a result of the resonance⁴.

To suppress the resonant tones, modern aircraft deploy passive devices when the bay doors open, such as porous fences along the leading edge of the cavity. Because the fundamental physics of the suppression device interaction with the cavity resonance mechanism and cavity flow is not fully understood, the design of the noise suppression device is based on prior experience and/or trial and error. Furthermore, the devices that suppress acoustic tones are known to affect the internal time-averaged flow patterns within the cavity, which can have either favorable or adverse effects on store separation characteristics depending on flight conditions. The trend toward lighter and more sophisticated ordnance increases the need for better understanding of actuator interaction with the flow environment in the cavity. The "cavity problem" is a

¹ Copyright©2002 by David R. Williams. Published by the American Institute of Aeronautics and Astronautics, Inc. with permission.

² Professor, Associate Fellow AIAA

challenge for flow control, because of the changing flow conditions during flight and the coupling of the cavity flow with store separation characteristics⁵.

Rossiter⁶ provided a description of the basic flow physics responsible for the resonance mechanism. As shown in Fig. 1, resonant modes may occur when the time for vortical wave propagation (vortex convection) matches with the time for an acoustic wave to travel upstream through the cavity. Although the mechanism is overly simple in that it does not account for cavity depth effects, shear layer thickness effects, and cannot predict disturbance amplitudes, the Rossiter equation has been reasonably successful in predicting the frequencies that are likely to appear.

All types of control techniques interfere in one way or another with the resonance mechanism. The Rossiter mechanism provides a starting point for understanding how resonant tones may be controlled through interference. Passive spoilers placed along the leading edge of the cavity act by thickening the shear layer and relocating the shear layer reattachment point downstream of the cavity wall. The latter effect reduces the amplitude of the acoustic feedback wave. Active flow control techniques have been explored recently as possible replacements for the passive approach⁷⁻¹². The injection of fluid into the cavity with blowing-type actuators is believed to delay the reattachment of the free shear layer. Open loop forcing of the shear layer excitation at frequencies in the inertial subrange have been shown to suppress Rossiter modes by modifying the turbulent energy cascade.^{12,13}

Passive and open-loop control techniques generally require large amounts of power either by an increase of cavity drag or through the actuator power requirements. Feedback control techniques have the potential to reduce tones with lower power, but are more complex than passive or open-loop control. Cattafesta, et al.⁹ demonstrated the efficiency in power that could be achieved with a feedback controller. Closed-loop techniques require three basic components: (1) flow state sensor, (2) control algorithm, and (3) actuator. Flow state sensors are typically either pressure sensors or microphones.

While the majority of recent work has focused on actuator development, equally important, but receiving less attention is the control algorithm. The potential benefits of using such an approach are an order of magnitude less actuator power requirement than open loop actuators, net cavity drag reduction, and adaptability to changing flight conditions.

In the first year we selected one type of flow state sensor (Kulite pressure transducer) and one type of actuator with zero net mass addition. Comparisons of different types of control systems were made to determine their efficacy in suppressing tones. The simplest was an analog control system with a manually adjusted gain and adjustable phase in the feedback loop. Digital controllers with various programmable algorithms, and an adaptive controller followed.

Even though progressively more sophisticated controllers were being used, the reduction in sound pressure level did not necessarily improve. Suppression levels of 18dB- 20dB were typical. For example, as feedback gain was increased to suppress a specific mode the acoustic energy would reappear at other frequencies in the spectrum. This phenomenon is known as “peaking” in the combustion community, e.g., Banaszuk, et al.¹⁴. Increasing the feedback gain would produce sideband peaks of energy about the mode being suppressed, which is known as “peak-splitting.” These two phenomena are illustrated for the cavity flow in Fig. 2.

Using a control algorithm based on flow field physics has several advantages. First it provides a framework for identifying flow “modules” in the resonance process, such as receptivity, scattering, etc. This approach ultimately leads to a better understanding of the flow phenomena by providing models of each component. Second, by using linear models the supposedly nonlinear effects can be isolated from linear effects. Third, the fundamental limits of controller performance can be determined. Knowledge of the fundamental limits on controller performance helps put an end to useless trial and error approaches. Finally, the linear model establishes a background for the introduction of more sophisticated low-order models, as discussed by Colonius¹⁵.

This paper provides details about the experiments, and is the companion to the paper by Rowley, et al.¹ in which details of the control are described. The experiments had two purposes: first to obtain data for identification of gains and phase delays associated with the components of the control model, and second to test the performance of the flow physics based model. The experimental setup is described in the next section. The results are discussed in section 3, and conclusions can be found in section 4.

2. Experimental Arrangement

The cavity control experiments were conducted in the Subsonic Wind Tunnel at the U.S. Air Force Academy. The wind tunnel has cross-section dimensions of 0.91m

x 0.91m (3 ft. x 3 ft.) It is capable of speeds up to $M = 0.6$, although the drag of the cavity limited the maximum Mach number to 0.55. The cavity model is the same used in previous experiments¹⁶. It was mounted in the floor of the wind tunnel test section, and had dimensions for the width $W = 0.38\text{m}$ (15 in.), and length $L = 0.51\text{m}$ (20 in.) The origin of the coordinate system was taken at the center, leading edge of the cavity with the x-axis in the streamwise direction. The spanwise coordinate is the z-axis, and the y-axis is normal to the plane of the cavity opening. Although the depth of the cavity could be varied, it was fixed in the present experiment at $D = 0.096\text{m}$ (4 in.) giving an aspect ratio $L/D = 5$.

The cavity was instrumented with eight Kulite sensors (model XCS-093) positioned from the front wall to the rear wall along the centerline of the cavity. The signals were bandpass filtered through fourth-order Butterworth filters with a passband of 0.4 Hz to 2.2kHz. All analog signals were sampled at 6,000 samples/(second-channel.)

Two hot-film probes were used with a Thermo-Systems Inc. IFA anemometer system to record velocity fluctuations in the shear layer.

3a. Control hardware

Both analog and digital control systems were used in the experiments. The analog control was a simple single input single output design with manually adjustable phase and gain on the feedback signal. The same system was used in previous experiments¹⁷, and provided a baseline for comparing the performance of control systems. The digital system allowed more flexibility in the control system design. Filters, time delays and gains could be set with much more precision and better repeatability than the analog system.

Analog Control

The single-input-single-output control used a Kulite pressure sensor as its input. The signal was narrow bandpass filtered about individual Rossiter modes with three Ithaco 4212 filters to create three feedback signals. Each feedback signal was phase-shifted through a manually adjusted circuit. The three signals were recombined with an adding circuit, and then sent to a 900 Watt Fender power amplifier to drive the actuator.

Digital Control

Recent developments in digital signal processor (DSP) technology have made it feasible to transition sophisticated digital control algorithms from the laboratory into practical flow control applications. The small size of DSP's and their low cost are attractive

features for applications on small aircraft. On board memory of order 100 kilowords and processing speeds at 75 mips are more than adequate to support algorithms fast enough to suppress tones in the kiloHertz range.

The digital control was built around a dSPACE ACE-1102 system, which simplifies programming of the DSP. A variety of different digital filters, plant models and control algorithms were programmed with Matlab[®] and Simulink[®]. The models could be directly downloaded into the DSP, which then acted as a standalone controller. The effective time step (or equivalent sample rate) of the DSP limits the bandwidth of the digital system, and this will depend on size of the algorithm. Larger programs run more slowly. In the present experiment the upper sample rate was limited to approximately 10,000 samples/sec. All Rossiter modes to be suppressed were less than 1,000 Hz, so the dSPACE system was sufficient.

Actuator

The actuator for both analog and digital systems consisted of a pair of 500 Watt, 8-inch Pyramid loudspeakers. The loudspeakers were enclosed in an aluminum housing to equalize the pressure surrounding the speaker cone with the wind tunnel test section pressure. Pressure equalization was essential to obtain good performance from the actuator. The actual power required by the actuators varied from 1 to 53 Watts depending on specific flow conditions. The transfer functions for the pressure and velocity responses of the actuator were measured with a hot-film anemometer and Bruel & Kjaer microphone, and are shown in Fig. 3a and Fig. 3b, respectively. The cutoff frequency of the actuator occurs at approximately 500 Hz.

4. Results

4a. Shear Layer Development

The shear layer development over the cavity is one of the primary elements of the resonance process. It determines the convective speed of the vortices (vortical waves), the growth rates and saturation amplitudes of the vortical waves. The shear layer acts like a filter/amplifier to the broadband turbulence from the boundary layer and feedback noise. Tam & Block¹⁸ discussed the importance of finite shear layer effects and incorporated it into their model of the cavity physics. They point out that shear layer growth rate is related to disturbance amplitude, and the two are coupled. Lacking detailed measurements they were forced to use an average value of the momentum thickness. Hankey & Shang¹⁹ used disturbance growth rates from stability theory to predict the relative amplitudes of the Rossiter modes. Detailed

measurements of a cavity shear layer were made by Kegerise²⁰ using hot-wire anemometers and a novel quantitative schlieren technique (optical deflectometry.) His experiments showed that the relative magnitudes of the Rossiter modes did not correspond to the predictions of linear stability theory, but were determined by the shear layer mode amplitudes at the downstream end of the cavity.

Measurements of the shear layer growth over cavities are somewhat limited. Sarohia²¹ studied the flow over an axisymmetric cavity and found momentum thickness growth rates to be as high as $d\theta/dx = 0.022$. Oster & Wygnanski²² studied the development of free shear layers (without a cavity) under forced and unforced conditions. Their results showed the growth rate of the unforced free shear layer depends upon the velocity ratio $r = U_1/U_2$. As the velocity ratio varied from $r = 0.3$ to 0.6 , $d\theta/dx$ decreased from 0.019 to 0.0085 . In the case of a shear layer forced with an oscillating flap Oster & Wygnanski found three separate regions of momentum thickness growth. Region I has a linear growth rate that exceeds the unforced case. In region II the growth rate slowed or even became negative at high forcing amplitudes. From flow visualization they determined that the normal vortex amalgamations are inhibited in region II. The growth rate in region III became linear again at a rate close to that in region I as vortex amalgamations reoccur.

Hot wire measurements of the shear layer velocity profiles are shown in Fig.4 for $x/L = 0.1$ to 0.6 . The y-coordinate is normalized by the vorticity thickness $\delta_{\omega} = (U_2 - U_1)/dU/dy|_{\max}$. The velocity deficit $U(y) - U_1$ was normalized by $(U_2 - U_1)$, where U_1 was determined to be approximately $0.12U_2$ by curvefits to the data. It is recognized that measurements of the low velocity region in the cavity are problematic due to the reversed flow. The corresponding r.m.s. velocity profiles are shown in Fig. 5.

Growth of the shear layer is shown in Fig. 6a. Analog control was used to suppress the resonant mode by 7dB. Essentially negligible difference is found between the forced and unforced cases. The data show a region of near zero growth between $x/L = 0.1$ to 0.2 , which is similar to region II found by Oster & Wygnanski. A comparison with free shear layer development ($r=0.3$) is made in Fig. 6b.

4b. Actuator input to shear layer

Open loop forcing experiments were conducted at $M=0.34$ to determine the response of the shear layer and cavity system to changing input amplitudes. The shear layer response was measured with a hot-film probe at $x/L = 0.031$, $y=0$. The forcing frequency was

fixed at 380 Hz. The linear response of the shear layer velocity responds to the voltage input to the actuator can be seen in Fig. 7a. The pressure response in the cavity relative to the velocity fluctuation level in the shear layer is shown in Fig.7b, and can be seen to have a nonlinear behavior.

4c. Shear layer

The cavity resonance process will selectively amplify specific modes that grow until an equilibrium limit-cycle state is reached. Since we are not conducting transient experiments, the data obtained occur with the shear layer in an equilibrium state. To be able to study the shear layer receptivity, the closed-loop control system is used to suppress the resonant mode. Simultaneously open-loop forcing with the actuator is used to inject a controlled disturbance at a frequency slightly detuned from the resonant mode. The development of the open-loop mode is then followed around the resonance loop in the cavity. For example, at $M=0.34$ the principal resonant mode occurs at 340Hz. This mode is suppressed by 10dB with the feedback controller, and then the actuator is driven in open loop at 380Hz. The 380Hz mode is detuned from the Rossiter resonance mechanism, hence it is not self-excited and does not saturate. Because the principal resonant modes are not completely suppressed, the detuned disturbances are developing on top of a flow field that is not in its pure base state. Nevertheless, as shown from the shear layer velocity profiles, the differences are not large between the suppressed state and the limit-cycle state.

The response of the shear layer is measured with the two hot-film probes located at $y=0$, $x/L = 0.031$ and 0.92 . The transfer function and phase as a function of the open-loop forcing signal are shown in Fig. 8. The shear layer shows higher gains at 220 Hz and 370 Hz than at the 340Hz principal Rossiter mode.

4d. Scattering –

The fluctuating vorticity field is converted into acoustic waves at the downstream end of the cavity. A comparison of downstream hot film signal with a nearby Kulite pressure transducer located in the downstream wall is shown in Fig. 9. Unfortunately, the acoustic feedback at the open-loop forcing frequency is also present in the pressure transducer signal, which contaminates the results to some degree and may explain the large gain at 340Hz.

4e. Acoustic feedback –

The upstream propagation of the acoustic waves was divided into the “reflection” and upstream propagation.

The reflection is a measure of the wave propagating from the downstream edge of the cavity to the floor of the cavity. In this experiment the distance was 127mm. The gain and phase for this component of the resonant loop are shown in Fig.10.

The transfer function for the upstream propagation of the acoustic waves in the cavity is plotted in Fig. 11. A monotonic increase in the transfer function with increasing frequency is observed. It is not known why the rapid changes in amplitude appear at frequencies above 350Hz. Finer resolution in the open-loop frequency increments will be needed to resolve the issue.

4f. Receptivity

Receptivity refers to the response of the shear layer to external disturbances, or to the conversion of acoustic disturbances into vortical waves in the shear layer. The shear layer receives input disturbances from at least three sources, namely the turbulent boundary layer, the feedback acoustic wave and the actuator. The boundary layer has a broad spectrum of vortical disturbances to drive the instability. In the cavity problem there is an additional input from the acoustic field to be considered. This includes the acoustic waves that feedback from the shear layer impinging on the downstream wall of the cavity. The third source in the case of control of cavity flows is from the actuator. The actuator introduces disturbances into the shear layer from the controller feedback path.

To obtain a measure of the receptivity transfer function it is necessary to separate the contribution from the actuator to the hot-film signal at the upstream end of the cavity. First the transfer function was computed with the pressure signal in the upstream wall as input, and the hot-film probe velocity signal at $x/L = 0.031$ as output. Next the output of the actuator was computed using the feedback voltage signal and the actuator transfer function to obtain the term to be subtracted from the first transfer function. The results are shown as the gain and phase corresponding to the open-loop forcing frequencies in Fig. 12.

6. Conclusions

Hot wire measurements of the shear layer development over a cavity showed similarities with forced free shear layer measurements. For comparison closed-loop control was used to suppress the resonant mode by 7dB, and no significant differences in shear layer development were found.

A novel approach to measuring transfer functions of the various flow components that make up the cavity resonance mechanism was attempted. Using

Rossiter's¹¹ model for resonance as a guide, the cavity flow was decomposed into five components representing 1) vortical waves in a shear layer, 2) scattering of vortices from the downstream edge to produce pressure waves, 3) reflection of the acoustic wave to the floor of the cavity, 4) upstream propagation of the acoustic wave through the cavity to the upstream wall, and 5) receptivity of the shear layer to the pressure waves. Closed-loop control was used to suppress the cavity resonance by 10dB. Simultaneously, open-loop forcing was used to introduce a new frequency into the shear layer. The response of the cavity components was documented in the form of transfer functions with phase plots as functions of the forcing frequency.

Acknowledgements

We are grateful for the support provided by the Air Force Office of Scientific Research through contract F49620-98-1-0276. The program was managed by Dr. Steven Walker. Actuator development at IIT was done by Mr. Byung-Hun Kim with partial support from the Aerospace Illinois: a NASA Space Grant Consortium. A special thanks goes to Mr. Ken Ostasiewski, Mr. Tim Hayden and SSgt. Buddy Johns for their invaluable assistance during the experiments over the last three years.

1. Rowley, C.W., Williams, D.R., Colonius, T., Murray, R.M., MacMartin, D. G., Fabris, D., "Model-Based Control of Cavity Oscillations, Part II: System Identification and Analysis," AIAA Paper 2002-0972, 40th Aerospace Sciences Meeting, Reno NV, January 2002.
2. Krishnamurty, K., "Acoustic radiation from two-dimensional rectangular cutouts in aerodynamic surfaces" N.A.C.A. Tech. Note 3487, August, 1955.
3. Roshko, A., "Some Measurements of Flow in a Rectangular Cutout," N.A.C.A. Tech. Note 3488, August, 1955.
4. McGregor, O.W., and White, R. A., "Drag of Rectangular Cavities in Supersonic and Transonic Flow Including the Effects of Cavity Resonance," AIAA J., **8**, 1970.
5. Pinney, M. A., and Leugers, J. E., "Experimental Investigation of the Impact of Internal/External Weapons carriage on a Generic Aircraft configuration," WL-TR-96-3110, Final Report, Wright Laboratory, 1996.
6. Rossiter, J.E., "Wind-Tunnel Experiments on the Flow over Rectangular Cavities at Subsonic and Transonic Speeds," Aeronautical Research Council Reports and Memo No. 3438, 1966.
7. McGrath, S. and Shaw, L., "Active Control of shallow cavity acoustic resonance," AIAA paper

- 96-1949, 27th AIAA Fluid Dynamics conference, New Orleans, June 1996
8. Shaw, L. and Northcraft, S., "Closed Loop Active Control for Cavity Acoustics," AIAA Paper 99-1902, June 1999.
 9. Cattafesta, L.N. III, Garg, S., Choudhari, M., Li, F., "Active Control of Flow-Induced Cavity Resonance," AIAA 97-1804, 28th Fluid Dynamics Conf. Snowmass Village CO, 1997.
 10. Raman, G., Envia, E., Bencic, T., "Tone Noise and Nearfield Pressure Produced by Jet-Cavity Interaction," AIAA paper 99-0604, 37th Aerospace Sciences Meeting, Reno NV, 1999.
 11. Fabris, D. and Williams, D.R., "Experimental Measurements of Cavity and Shear Layer Response to Unsteady Bleed Forcing," AIAA paper 99-0605, 37th Aerospace Sciences Meeting, Reno NV, 1999.
 12. Stanek, M.J., Raman, G., Kibens, V., Ross, J.A., Odedra, J., and Peto, J.W., "Control of Cavity Resonance Through Very High Frequency Forcing," AIAA Paper 2000-1905, 6th AIAA/CEAS Aeroacoustics meeting, Lahaina, HA, June 2000.
 13. Stanek, M.J., Raman, G., Kibens, V., Ross, J.A., Odedra, J., Peto, J., "Suppression of Cavity Resonance Using High Frequency Forcing-The Characteristic Signature of Effective Devices," AIAA Paper 2001-2128, 7th AIAA/CEAS Aeroacoustics Conf., Maastricht, Netherlands, May 2001.
 14. Banaszuk, A., Mehta, P.G., Jacobson, C.A., Khibnik, A.I., "Limits of Achievable Performance of Controlled Combustion Processes," IEEE Trans. Automat. Contr. (submitted), 2001.
 15. Colonius, T., "An Overview of Simulation, Modeling, and Active Control of Flow/Acoustic Resonance in Open Cavities," AIAA Paper 2001-0076, 39th Aerospace Sciences Meeting, Reno NV, January, 2001.
 16. Williams, D. R., Fabris, D., Iwanski, K., Morrow, J., "Closed loop control in cavities with unsteady bleed forcing," AIAA Paper 2000-0470, 38th Aerospace Sciences Meeting and Exhibit, Reno NV, January 2000.
 17. Williams, D.R., Fabris, D., Morrow, J., "Experiments on controlling multiple acoustic modes in cavities," AIAA Paper 2000-1903, 6th Aeroacoustics Conf., Lahaina, HA, June 2000.
 18. Tam, C.K.W. and Block, P.J.W., "On the tones and pressure oscillations induced by flow over rectangular cavities." *J. Fluid Mech.* 89(2) pp373-399, 1978.
 19. Hankey, W.L. and Shang, J.S., "Analysis of pressure oscillation in an open cavity." *AIAA J.* 18(8) pp892-898, 1980.
 20. Kegerise, M.A., "An Experimental Investigation of Flow-Induced Cavity Oscillations," Ph.D. Dissertation, Syracuse University, 1999.
 21. Sarohia, V., "Experimental Investigation of Oscillations in Flows Over Shallow Cavities," *AIAA J.*, 15 pp984-991, July 1977.
 22. Oster, D. and Wygnanski, I., "The forced mixing layer between parallel streams," *J. Fluid Mech.* 123 pp91-130, 1982.

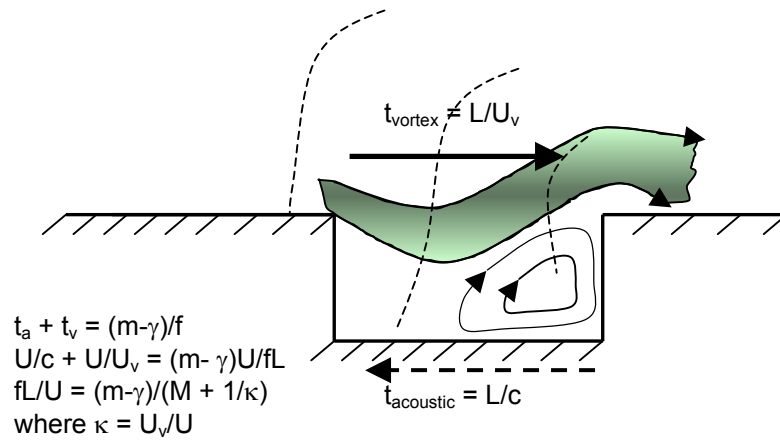


Fig. 1 – Schematic of Rossiter’s resonance mechanism. Vortical waves convect downstream in the shear layer, while acoustic waves propagate upstream in the cavity.

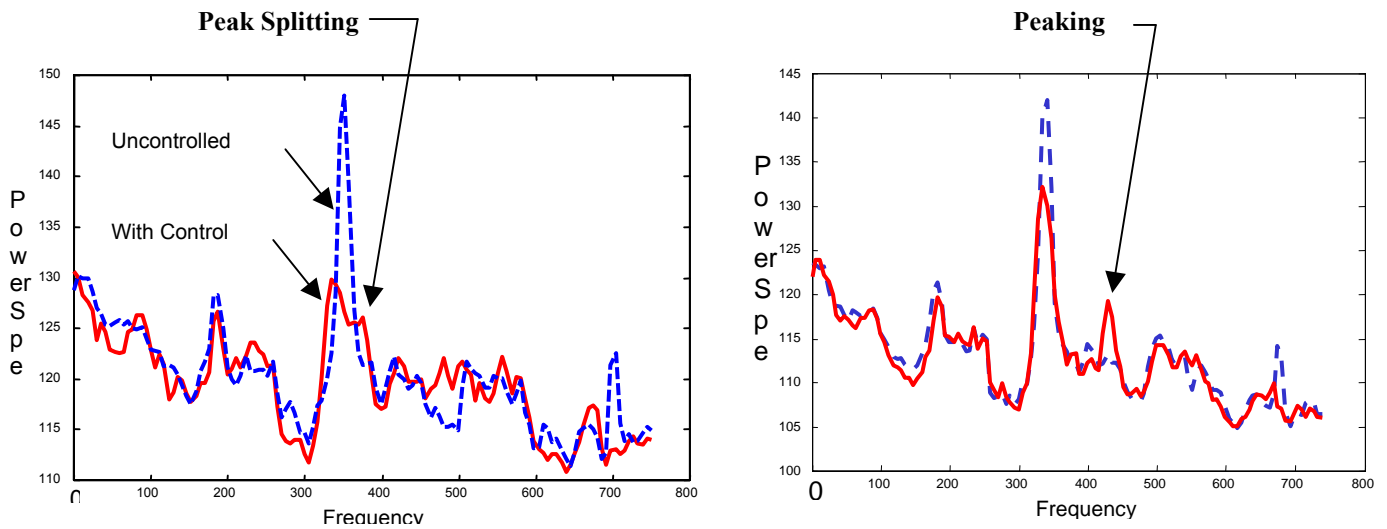


Fig. 2 – Examples of “peak splitting” and “peaking” phenomena that limit the effectiveness of closed-loop controllers.

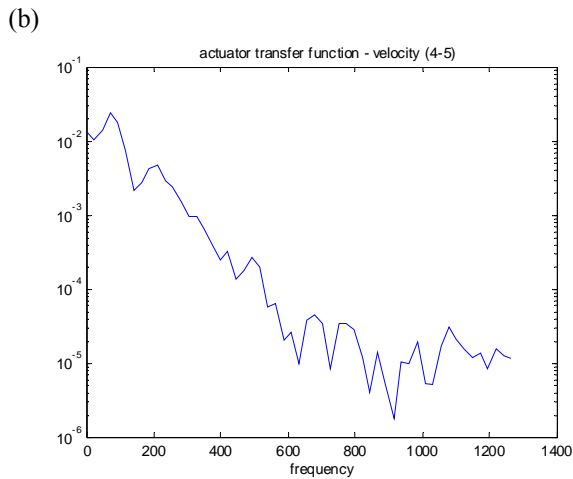
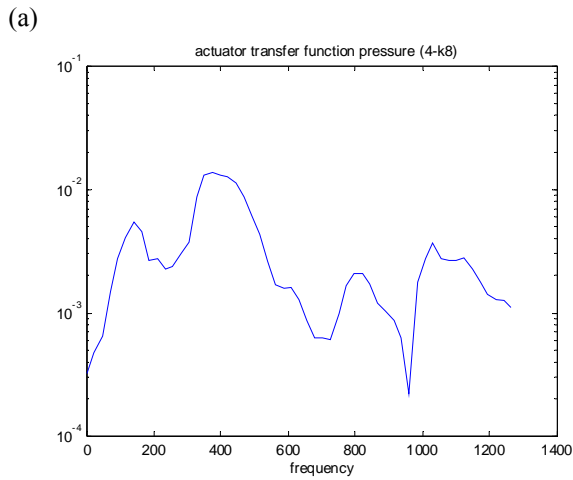


Fig. 3. Transfer functions obtained between voltage input signal to actuator and output signals measured by pressure sensor and hot-film probe. (a)- pressure sensor on upstream wall, K8. (b)- hot-film at $x/L = .031$. A small width nozzle was used in this experiment ($w = 3/16''$) compared to $w=1/2''$ in earlier studies. The effect was to reduce the actuator cutoff frequency from 600Hz to 500Hz.

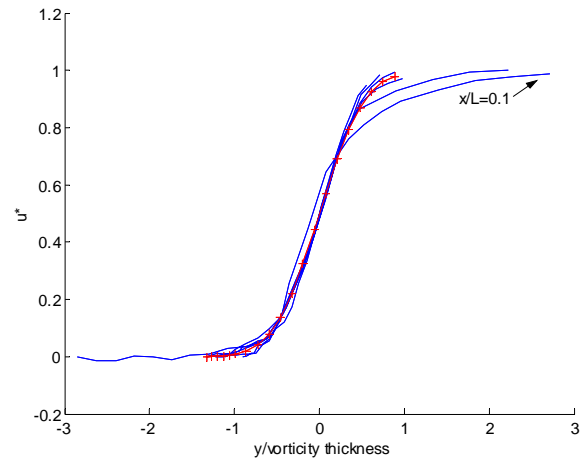


Fig. 4 – Normalized mean velocity profiles from $x/L = 0.1$ to $x/L = 0.6$, $M = 0.35$. The y -coordinate is normalized by the vorticity thickness. The normalized velocity is $u^* = (U(y)-U_1)/(U_2 - U_1)$.

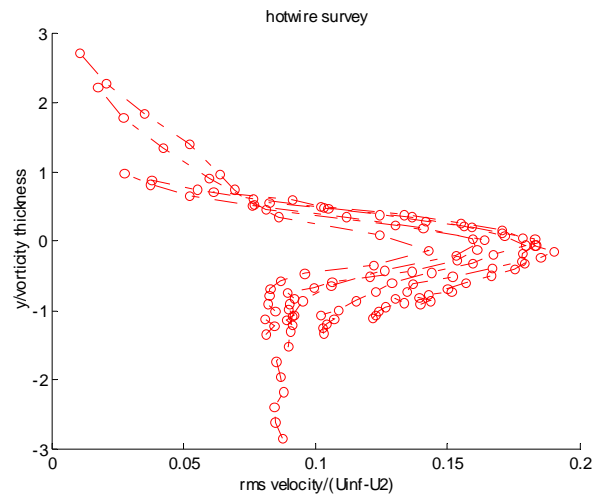


Fig. 5 – Fluctuating velocity profiles with the y -coordinate normalized by the vorticity thickness.

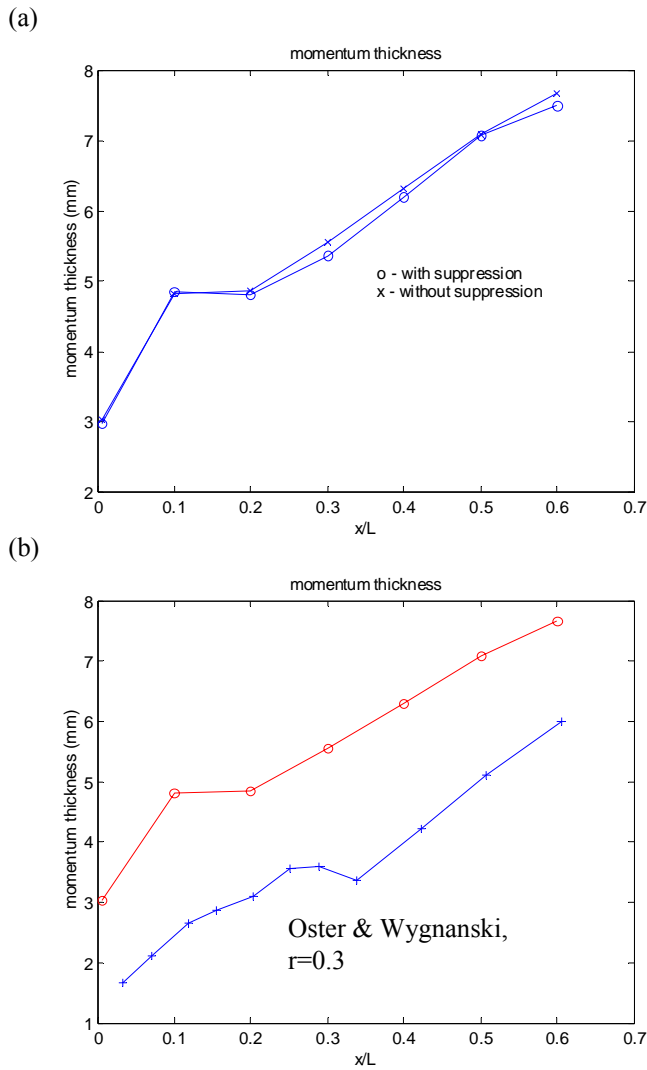


Fig. 6 – Streamwise variation of the shear layer momentum thickness, $M = 0.35$. (a) comparison of growth rate with and without suppression of acoustic tones. Suppression had only a small effect on the shear layer development. (b) Comparison of growth with the Oster & Wygnanski forced shear layer results. Both show a flat region II.

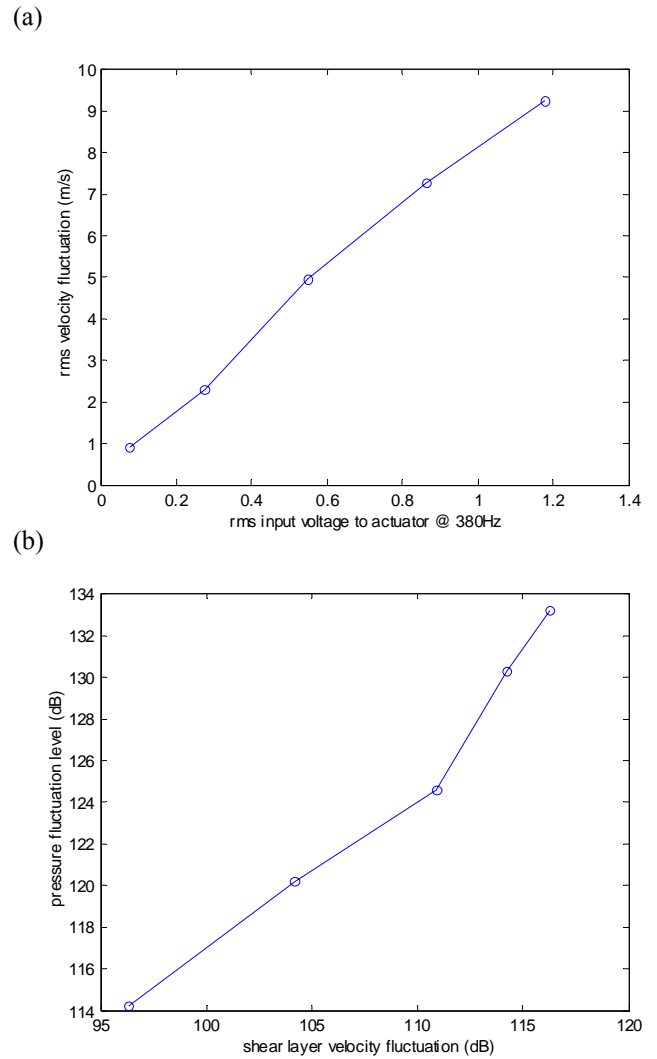


Fig.7 – Dependence of shear layer velocity fluctuation amplitude on voltage input to the actuator. Sound pressure level in cavity at 380 Hz dependence on initial shear layer velocity fluctuation amplitude.

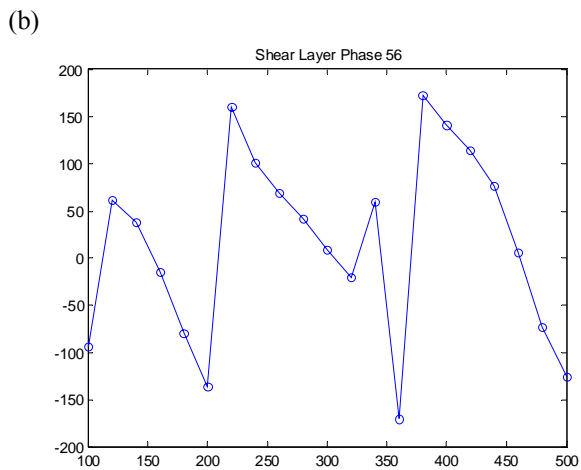
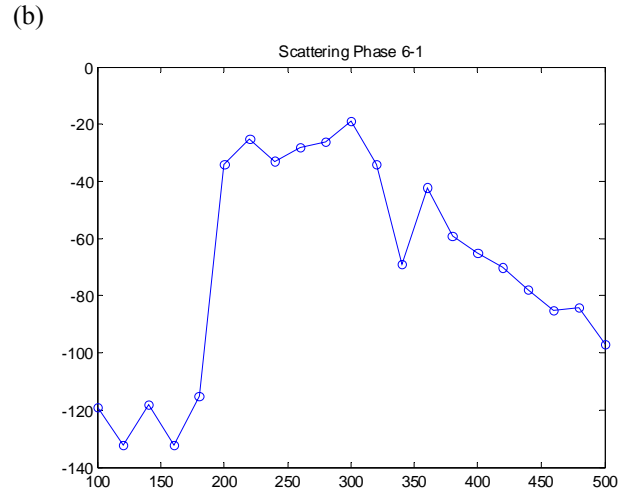
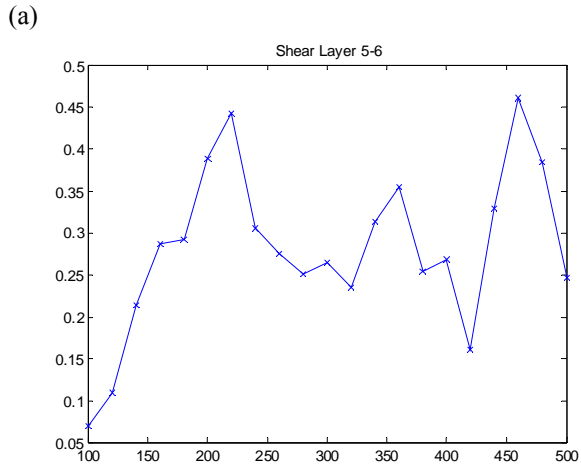


Fig. 9 – Scattering transfer function with phase obtained with open loop forcing between the downstream hot film probe and pressure transducer in downstream wall. (a) transfer function; (b) phase.

Fig. 8 – Shear layer transfer function with phase obtained with open loop forcing. (a) transfer function; (b) phase.

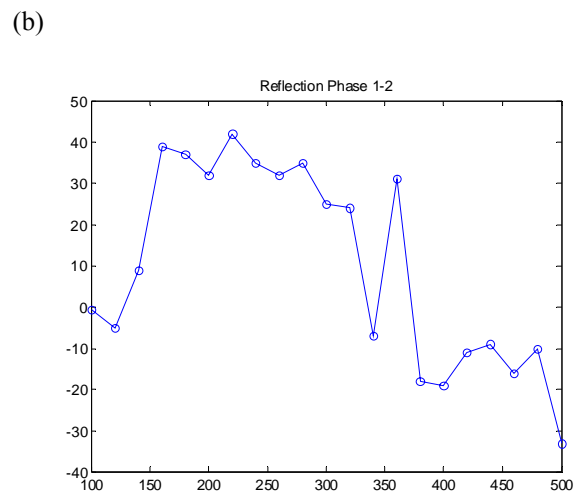
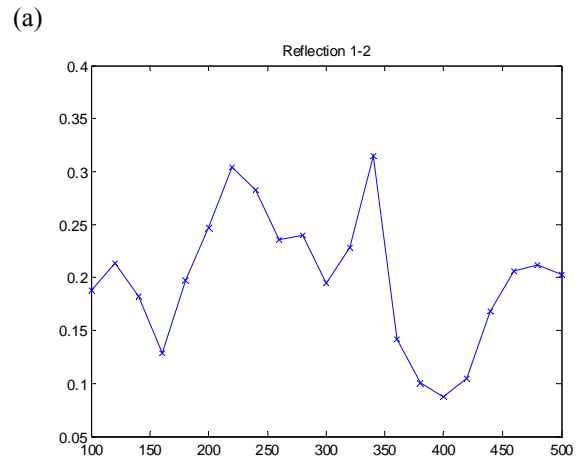
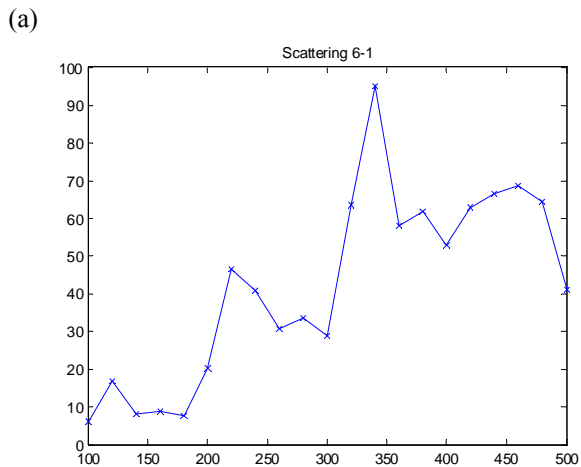


Fig. 10 – Reflected wave from downstream edge of cavity to floor. (a) transfer function; (b) phase.

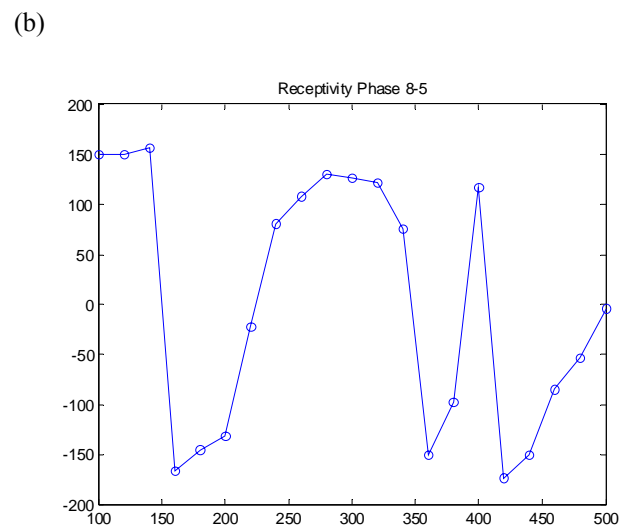
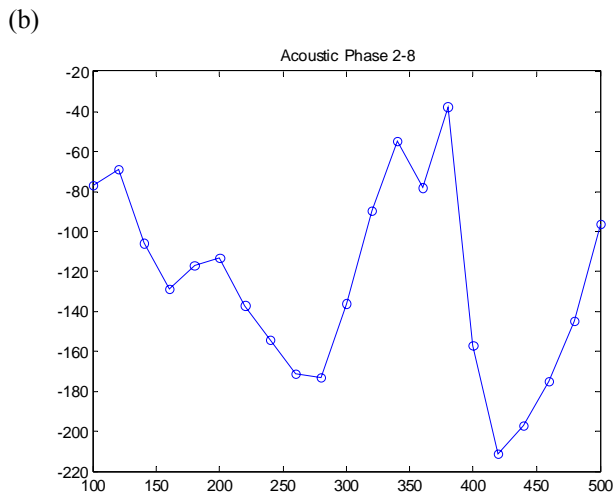
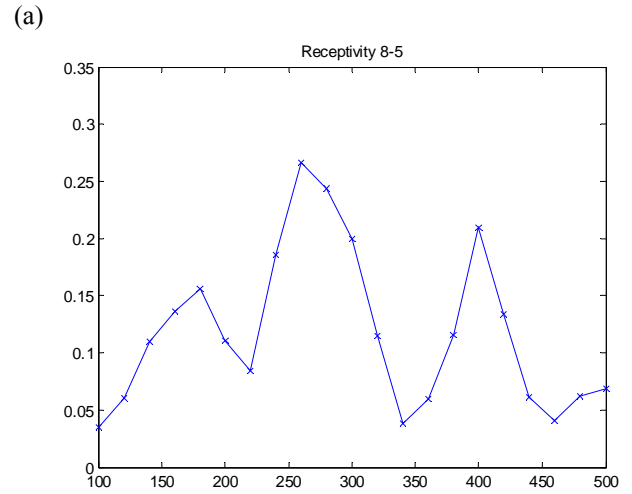
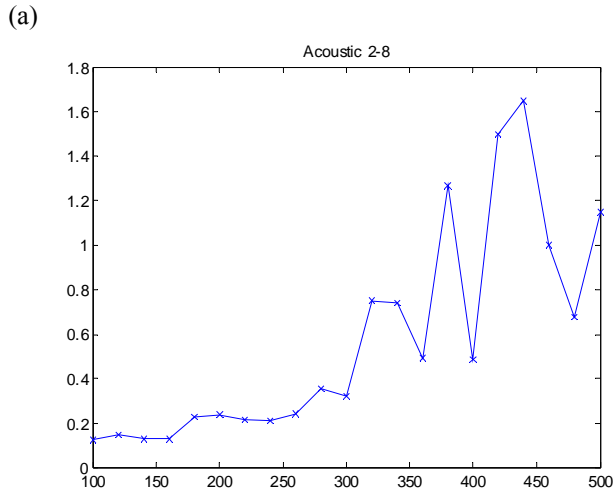


Fig. 11 - Transfer function of upstream propagating acoustic wave.

Fig. 12 – Leading edge receptivity measured between pressure transducer in the upstream wall and a hot-film probe located in the shear layer. (a) transfer function; (b) phase.